Supplementary information for:

In situ Assembly of Active Surface-Enhanced Raman Scattering Substrates *via* Electric Field-Guided Growth of Dendritic Nanoparticle Structures

Hannah Dies, Joshua Raveendran, Carlos Escobedo, Aristides Docoslis*

Department of Chemical Engineering, Queen's University, Kingston ON Canada K7L 3N6

*To whom correspondence should be addressed:

Prof. Aris Docoslis, PhD, PEng

Tel: 1-613-533-6949

Fax: 1-613-533-6637

Email: docoslis@queensu.ca

Table of Contents

The properties of water and silver nanoparticles used for numerical simulations are summarized in Table S*1*. The conductivity of the aqueous citrate buffer was measured using a Malvern Zetasizer ZS system (Malvern Instruments Ltd.).

Table S1: Various properties of water and silver nanoparticles used for simulations.

Property	Water	Silver nanoparticle
Viscosity (mPa*s)	0.89[1]	N/A
Relative permittivity, ϵ_r	80[1]	/
Relative permittivity, ϵ' (546nm)	/	-9.9613[2]
Relative permittivity, ϵ'' (546nm)	/	0.91377[2]
Conductivity (mS/m)	59.3	/

Numerical Simulations

A cylindrical quadrant was used to perform the simulations. For simulations involving fluid flow, a larger control volume was used to ensure edges effects were minimized. The dimensions of both control volumes are summarized in Table S2 and are displayed in Figure S1.

Table S2: Dimensions of the simulated control volumes.

Dimension	Nanoparticle Present Model	Fluid Flow Model
Radius (μm)	190	250
Fluid Height (μm)	20	100
Electrode thickness (μm)	0.1	0.1

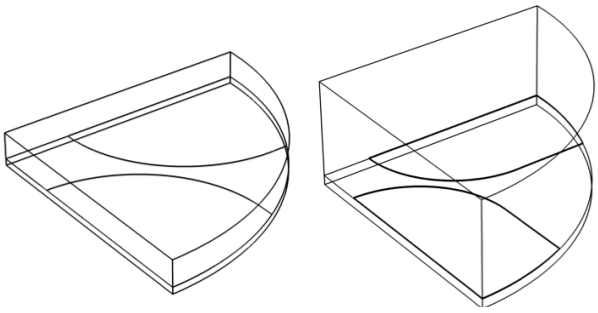

Figure S1: Control volumes which were used to perform simulations. Model on the left was used when nanoparticle was present while model on the right was used to calculate fluid flow.

Electrical Domain

To account for the presence of the electrical double layer (EDL) and the shielding it provides, the coefficient form of the partial differential equation was used to solve for the electric field. The EDL was assumed to be in a quasi-equilibrium and was treated as a boundary layer with respect to the fluid in the bulk. The EDL was modelled as a capacitor whereas the bulk fluid acted as a resistor.[3] The potential in the bulk of the fluid can be described using Gauss's law.

$$\nabla \cdot (-\epsilon_{\mathrm{m}} \nabla V) = \rho_E \qquad \text{(S1)}$$

Assuming in the bulk of the fluid there is not net body charge density ($\rho_E = 0$) and the fluid has a constant dielectric constant ($\nabla \cdot \epsilon_m = 0$), Gauss's law can be simplified to the Laplace equation.

$$\nabla^2 V = 0 \qquad \text{(S2)}$$

The charging of the EDL and boundary between the EDL and fluid in the bulk can be described using the charge balance (equation S3) if lateral currents along the EDL are negligible compared to normal currents and there is a small voltage drop in the diffuse layer ($\Delta\phi_d < \frac{k_B T}{q} = 0.025V$).[3]

$$n \cdot \nabla V = \frac{i\omega C_{DL}}{\sigma_m}(V - V_{app}) \qquad \text{(S3)}$$

where n is a unit normal vector, σ_m is the conductivity of the fluid, C_{DL} is the capacitance per unit area for the EDL, V_{app} is voltage applied to the electrodes and ω is the angular frequency of the applied voltage. The C_{DL} can be approximated using a ratio of the fluid's dielectric constant and the Debye length ($C_{DL} \approx \frac{\epsilon_m}{\lambda_D}$) with the Debye length calculated using equation S4.[3]

$$\lambda_D = \sqrt{\frac{\epsilon_m k_B T}{2z^2 q^2 c_o N_a}} \qquad \text{(S4)}$$

where k_B is the Boltzmann constant, T is the temperature, z is the valency of ions, q is the elemental charge, c_0 is the concentration of ions in the bulk and N_a is Avogadro's number. The silicon dioxide substrate and outer fluid walls were described as an insulating surface ($n \cdot \nabla V = 0$). The electrodes were set to be 180^0 out of phase with one another, with one electrode receiving an applied voltage of 1.5V and the other -1.5V to simulate $3V_{peak\text{-}peak}$. Simulations which incorporated a nanoparticle had the nanoparticle act as an extension of the electrode (attached to electrode with same applied voltage but different material) with equation S3 also applied to the nanoparticle surface.

Fluid Domain

The fluid domain was simulated after solving for the electrical domain. The fluid flow in the control volume was calculated by solving both the continuity equation and a simplified Navier-Stokes equation (inertial term neglected). The fluid was assumed to be incompressible.

$$\nabla \cdot \boldsymbol{v} = 0 \qquad \text{(S5)}$$

$$\eta \nabla^2 \boldsymbol{v} = \boldsymbol{\nabla} \mathrm{p} \qquad \text{(S6)}$$

where, $\boldsymbol{v}$ is the fluid velocity, η is the viscosity of the fluid and p is the pressure. The electrode surface had a tangential slip velocity applied to it to incorporate alternating current electro-osmosis based on a modified Helmholtz-Smoluchowski equation.[3]

$$\boldsymbol{v}_{slip} = \frac{1}{2}\frac{\epsilon_m \Lambda}{\eta} Re\{(V - V_{app})\boldsymbol{E}_t^*\} \qquad \text{(S7)}$$

where Λ is a correction factor equal to the ratio of the capacitance of the stern layer relative to the capacitance of the complete EDL, V is the potential outside the EDL and $\boldsymbol{E}_t^*$ is the complex conjugate of the tangential component of the electric field along the surface of the EDL. A no slip condition ($\boldsymbol{v} = 0$) was applied to the silicon surface. The outer fluid walls had a zero normal velocity ($n \cdot \boldsymbol{v} = 0$).

Schematic diagrams shown below (Figures S2 and S3) summarize the domain and boundary conditions used to simulate the electrical and fluid domain.

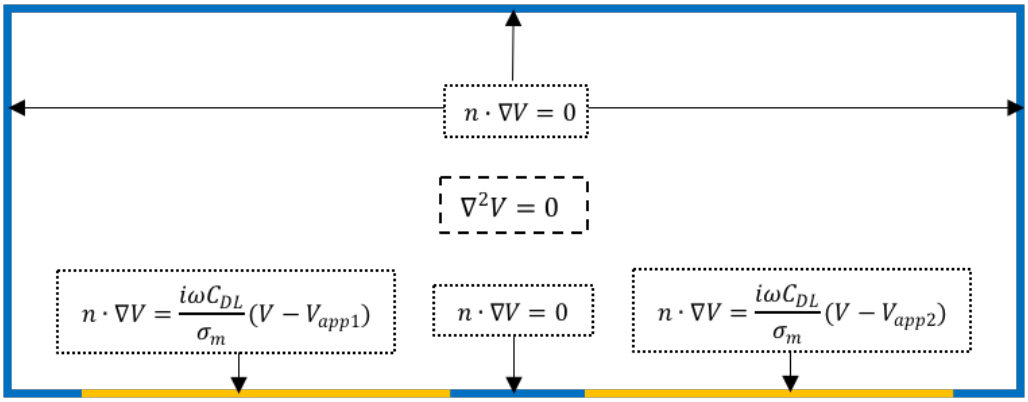

Figure S2: Schematic diagram of governing equations and boundary conditions used to solve electrical domain to determine electrical potential and field within control volume.

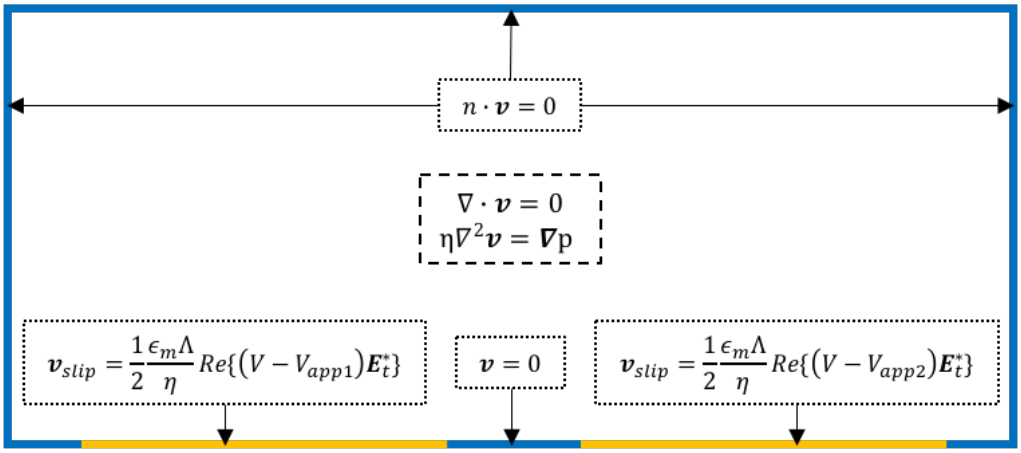

Figure S3: Schematic diagram of governing equations and boundary conditions used to solve fluid domain to determine fluid flow within control volume.

Spectra Collected

Spectra presented in manuscript were filtered and baseline corrected. A series of comparison figures are shown below; showing both the corrected spectra and the raw spectra collected for several different analytes.

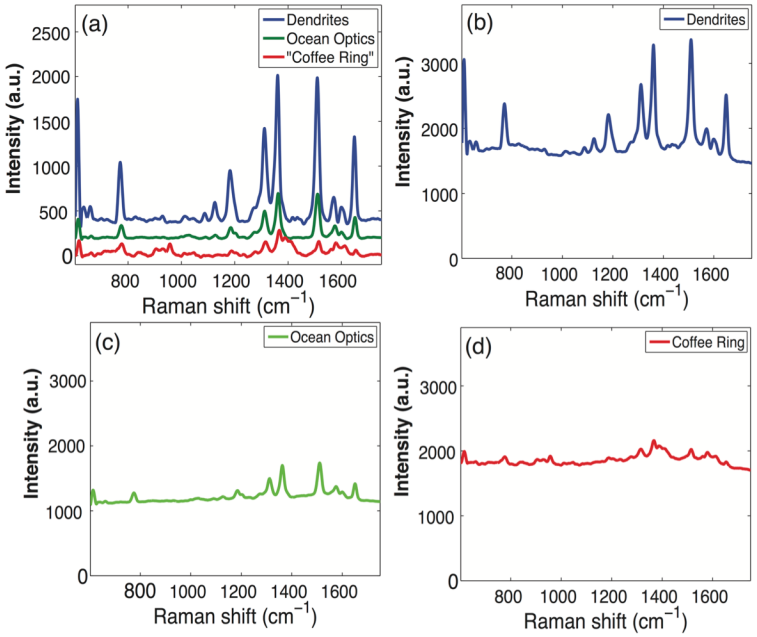

Figure S4: (a) Comparison of 10^{-5}M R6G SERS spectra on three different substrates after being baseline corrected. Spectra are shifted along vertical axis for visualization. (b) Raw spectrum of R6G collected on Ag dendrites. (c) Raw spectrum of R6G on Ocean Optics Au SERS substrates. (d) Raw spectrum of R6G on Ag substrate deposited using passive evaporation.

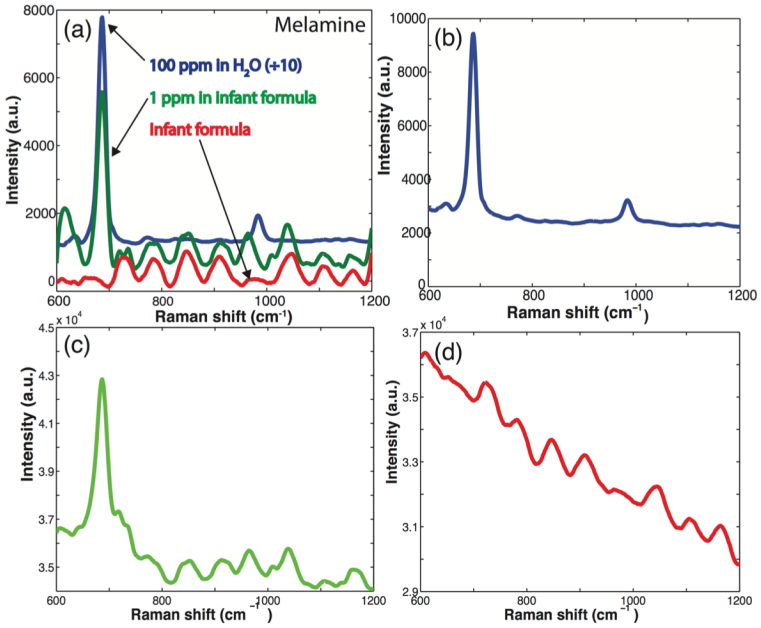

Figure S5: (a) SERS spectra of melamine in 2 different mediums and SERS spectrum from infant formula after being baseline corrected and filtered. (b) Raw spectrum of melamine in water (100ppm). (c) Raw spectrum of melamine in infant formula after purification and isolation (1ppm). (d) Raw spectrum of infant formula that has not been spiked melamine but has gone through same purification process.

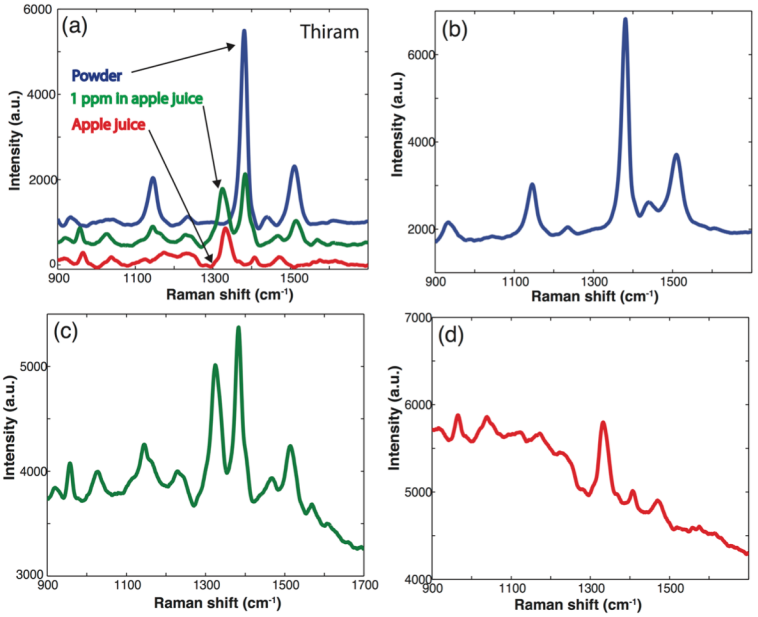

Figure S6: (a) SERS spectra of thiram both as a powder and in apple juice along with spectrum of apple juice after being baseline corrected and filtered. (b) Raw spectrum of thiram as a powder. (c) Initial spectrum of apple juice which has been spiked with thiram (1ppm). (d) Raw spectrum of non-contaminated apple juice.

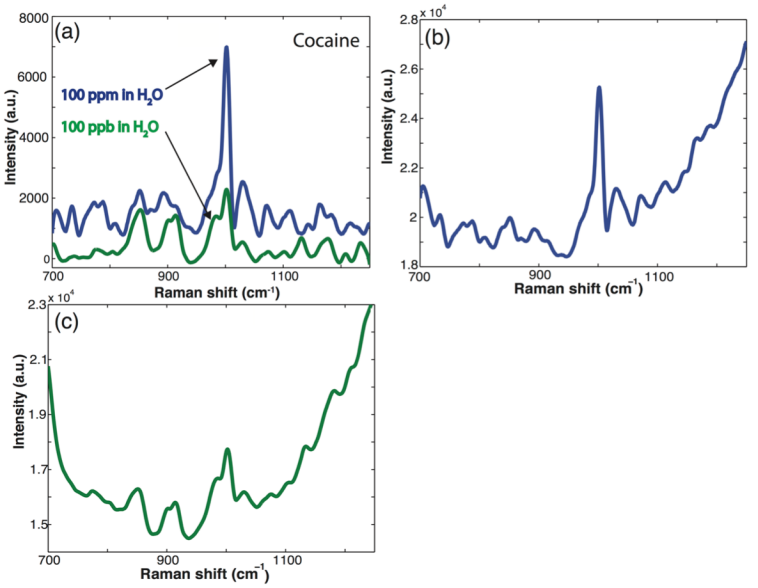

Figure S7: (a) SERS spectra of cocaine in water at 100 ppm and 100 ppb. (b) Raw spectrum of cocaine at 100 ppm. (c) Raw spectrum of cocaine at 100 ppb.

References

1 J. M. Smith, H. C. Van Ness and M. M. Abbot, *Introduction to Chemical Engineering*

Thermodynamics, McGraw-Hill Companies, Inc, Boston, seventh ed., 2005.

2 A. D. Rakic, A. B. Djurišic, J. M. Elazar and M. L. Majewski, *Appl. Opt.*, 1998, **37**, 5271–5283.

3 N. G. Green, A. Ramos, A. Gonzalez, H. Morgan and A. Castellanos, *Phys. Rev. E*, 2002, **66**, 1–11.